

Extending The Methodology Of X-ray Crystallography To Allow X-ray Microscopy Without X-ray Optics

Jianwei Miao^{*}, Pambos Charalambous[†], Janos Kirz^{*} & David Sayre^{*}

^{*} *Department of Physics & Astronomy, State University of New York,
Stony Brook, New York 11794-3800, USA*

[†] *Kings College, Strand, London WC2R 2LS, UK*

Abstract. We demonstrate that the soft X-ray diffraction pattern from a micron-size non-crystalline specimen can be recorded and inverted to form a high-resolution image. The phase problem is overcome by oversampling the diffraction pattern. The image is obtained using an iterative algorithm. The technique provides a method for X-ray microscopy requiring no high-resolution X-ray optical elements or detectors. In the present work, a resolution of approximately 60 nm was obtained, but we believe that considerably higher resolution can be achieved.

1. INTRODUCTION

X-ray microscopy is a well-established technique to image micron-size specimens at submicron resolution^{1,2}. The resolution of the technique is limited by the resolution of the X-ray optics -- commonly a zone plate -- and, for biological specimens, the radiation damage. While the radiation damage problem can be mitigated somewhat by using cryogenic techniques, the resolution of the zone plate is limited by fabrication difficulties. At present, the highest resolution achievable is around 30 - 50 nm^{3,4}. To get considerably higher resolution, much shorter wavelength particles such as electrons are needed for imaging. While an electron microscope can achieve less than 1 nm resolution, it can only study thin (< 0.5 μm) specimens due to the penetration length and contrast mechanism of the electrons. To obtain even higher resolution, X-ray crystallography is employed which needs not only short wavelength X-rays, but also crystalline specimens. Constructive interference among the large number of identical unit cells generates strong Bragg peaks by which X-ray crystallography can achieve atomic resolution without serious radiation damage to the specimens. Although X-ray crystallography becomes such a powerful technique to image specimens both in material science and structural biology, it is only applicable to crystalline specimens, while most biological specimens, for example, can not be or are too big to be crystallized. That the methodology of X-ray crystallography may be extended to non-crystals was first proposed by Sayre in 1980⁵. This extension, by combining X-ray Crystallography with X-ray Microscopy, eliminates the necessity of crystallization and high resolution X-ray optics. Although in principle this technique can obtain three-dimensional image of whole biological cells and complex sub-cellular biological specimens at high resolution, it faces two challenges. Firstly, when the specimen is non-crystalline, the diffraction pattern is faint and continuous, which poses the challenge to record such a diffraction pattern^{6,7}. The second challenge is the

well-known 'phase problem', the usually unavoidable loss of the phase information in the diffraction intensity. It was not until recently that we reported the first successful recording and reconstruction of the diffraction pattern from a non-crystalline specimen⁸. We report here detailed information of our experiment and a second successful reconstruction at higher resolution with less reconstruction time.

2. RECORDING THE DIFFRACTION PATTERN

Our experiment was performed at the X1A beamline at the National Synchrotron Light Source (NSLS). We used an entrance slit, grating and exit slit to select monochromatic X-rays. The widths of the entrance and exit slits were set at 40 and 23 μm , respectively, which corresponds to a resolving power of about 850 for soft X-rays with $\lambda = 1.7 \text{ nm}$. Our experimental chamber, as Fig. 1 shows, was mounted about 80 cm downstream of the exit slit. The first element inside the chamber was a 10 μm pinhole which was used to generate a small, collimated beam and also assured spatial coherence. The pinhole could be manually adjusted by an X-Y stage mounted outside of the chamber. To limit the effect of the scatter from the edge of this pinhole, the specimen was placed only about 30 μm from the corner of the silicon nitride membrane, allowing the silicon support to protect three quadrants of the detector from the scatter. The silicon nitride membrane was mounted on a commercial cryogenic sample holder. The holder could be manually adjusted in both the X and Y direction and could also be rotated by the stages outside the chamber. The detector, a back-thinned, liquid nitrogen cooled CCD with 512 x 512 pixels and a 24 μm x 24 μm pixel size, was placed downstream of the specimen at a distance of 25 cm. To position the specimen to the small beam spot, an optical microscope mounted above the chamber was used for coarse alignment and the CCD detector for fine alignment. In front of the CCD detector was a 220 μm in diameter wire which was used as beam stop and could be adjusted both in the X and Y direction. A photodiode could be inserted between the beam stop and the CCD to monitor the beam intensity in the presence or absence of pinhole, beam stop and specimen, and to help to align these components in the beam. The entire chamber was in vacuum with pressure around 10^{-5} torr and an air-lock for rapid sample change.

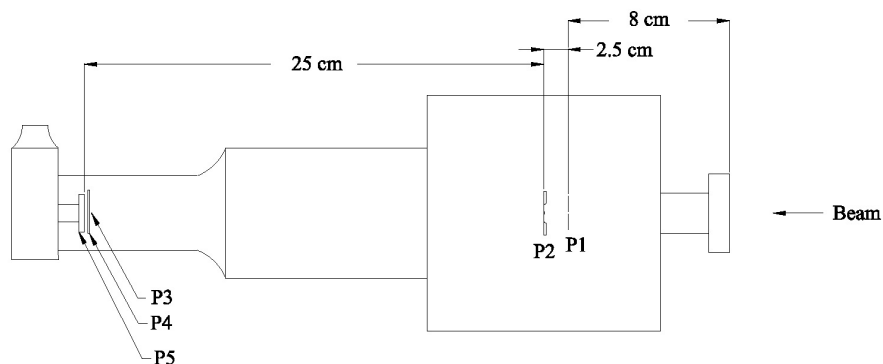


FIGURE 1. Schematic layout of the diffraction chamber. P1: Pinhole, P2: Specimen, P3: Central Stop, P4: Photodiode, and P5: CCD.

By using this setup, we studied a non-crystalline test specimen. The specimen was a collection of gold dots, each ~ 100 nm in diameter and 80 nm thick, deposited on a 100 nm thick silicon nitride membrane, to form a set of six letters. Fig. 2a shows a Scanning Transmission X-ray Microscopy (STXM) image of the specimen. The image was recorded on the X1A beamline at the NSLS. Fig. 2b is a diffraction pattern of the specimen, in which the fourth-quadrant data were obtained by using central symmetry. Since the central region was obscured by the beam stop, we replaced the central area of the X-ray diffraction pattern by a patch consisting of the low-resolution part of the squared magnitude of the Fourier transform of the STXM image of Fig. 2a. The patch, a circular area with a 19-pixel radius area, occupies less than 0.5% of the whole diffraction pattern. The pattern with exposure time of about 5 min extends to the edge of the CCD, suggesting that a larger detector would directly lead to higher spatial resolution.

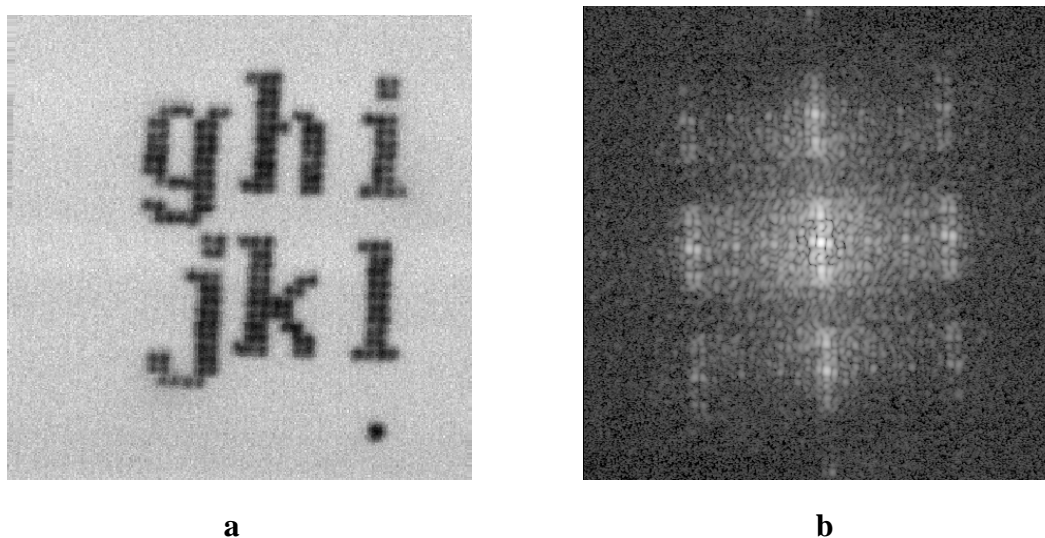


FIGURE 2 **a.** A STXM image of the specimen, **b.** A diffraction pattern of the specimen (using a logarithmic scale).

3. RECONSTRUCTING THE DIFFRACTION PATTERN

The intensity of the diffraction pattern provides a record of the magnitude, but not the phase, of the structure information. To invert an image from the diffraction pattern, one faces therefore the phase problem. The situation for the non-crystalline specimens is different, however, in that the diffraction pattern is faint and continuous instead of a collection of discrete Bragg peaks. This continuous pattern can therefore be sampled on a finer scale. That the oversampling technique may lead to the phase information was first suggested by Bates⁹. Most recently, we made progress in understanding the applicability of the oversampling technique to the phase problem. We proposed a theory to explain the oversampling technique and showed that Bates's criteria can be relaxed somewhat for the higher-dimensional cases¹⁰⁻¹². To apply the oversampling technique for the phase retrieval, we developed an iterative algorithm by modifying

Fienup's¹³. Each iteration of the algorithm consists of the following steps. From the magnitude of the Fourier transform and a guessed set of phases (a random set phase for the initial iteration), a Fourier transform pattern can be obtained. By applying inverse Fourier transform to the pattern, we get an image in the real space. We then enforce two kinds of constraints on the image; (i). If the diffraction pattern is oversampled, we define a finite support based on the oversampling degree, and drive the pixel value outside of the support close to zero. (ii). Inside the finite support, positivity constraints are enforced either on the real part or the imaginary part. After these processes, a new image is generated. By applying Fourier transform on the new image, we get a new pattern in the Fourier space. We adopt the phases from the pattern (also restoring the phase of the central pixel to zero) and thereby obtain a new guessed phase set. Usually, after a few hundred iterations, the correct phase set is retrieved. For detailed information, one may refer to previous publications^{6, 10-12}.

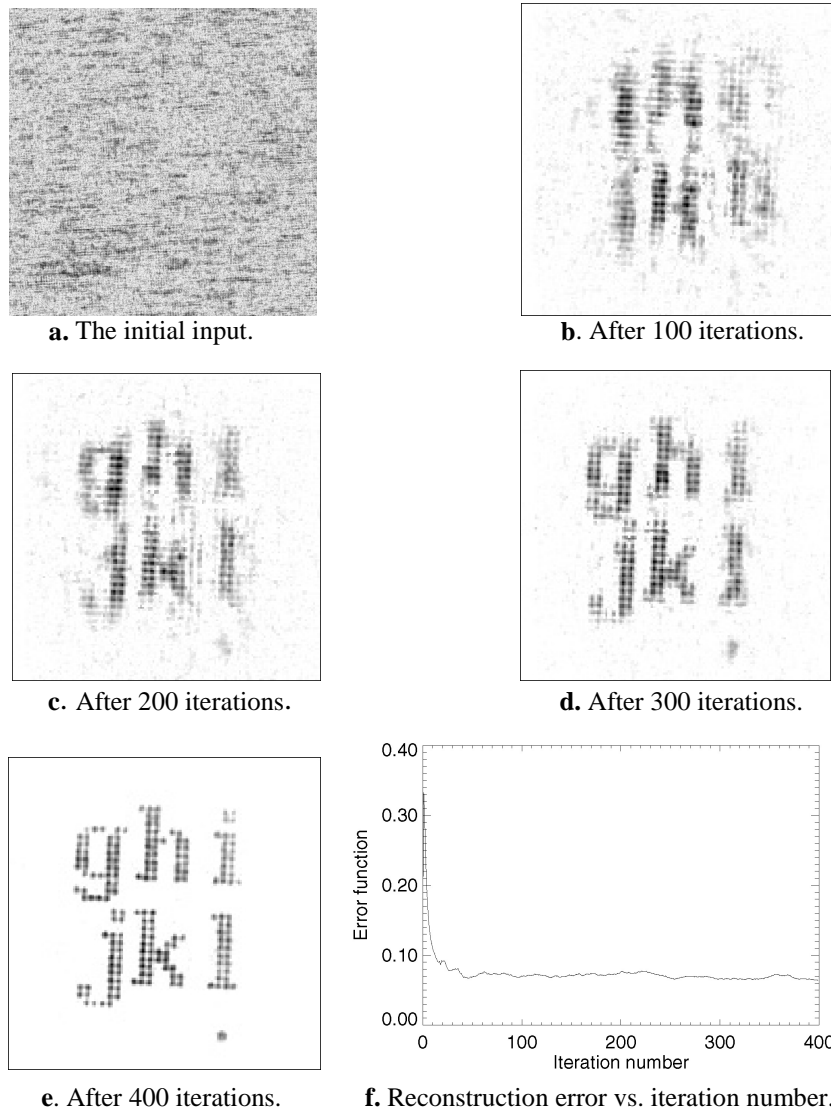
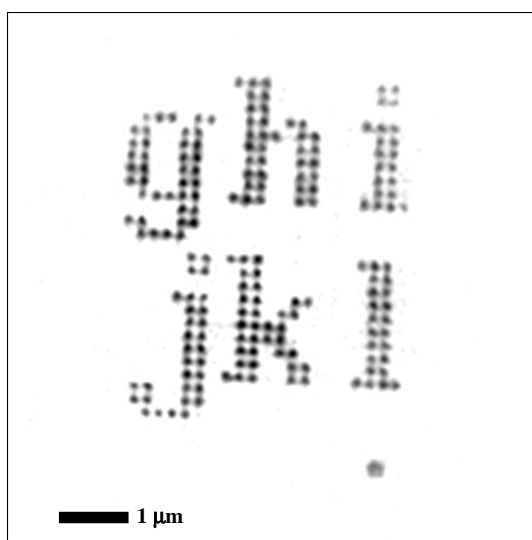


FIGURE 3. The convergence of a reconstruction.

By employing the algorithm mentioned above, we reconstructed the diffraction pattern of Fig. 2b. Fig. 3 shows the convergence of a reconstruction with a finite support of a $7.5 \mu\text{m} \times 7.5 \mu\text{m}$ square. Fig. 3a is an image processed from the experimental diffraction pattern and a random phase. Figs. 3b, 3c, 3d and 3e show the reconstructions after 100, 200, 300 and 400 iterations, respectively. Interestingly, the image was rotated 180° between Figs. 3b and 3c. This is due to the fact that one can not distinguish a phase and its conjugate from a diffraction pattern alone. Fig. 3f shows the convergence of the reconstruction error vs. the iteration number. The error function was defined as the ratio of the sum of the pixel values outside the finite support to the sum of the total pixel value¹⁰. Since the image reconstructed from an oversampled diffraction pattern was confined inside the finite support, the error function of a correct phase should be zero for a noise free diffraction pattern, but was only close to zero for an experimental pattern. Fig. 3f implies that the reconstruction



converged very fast during the first 50 iterations, and more slowly after that. After 400 iterations, a high quality image (Fig. 4) was obtained. The computing time of 400 iteration is ~ 15 min on a 450 MHz Pentium II workstation. Fig. 4, the same image as Fig. 3e but interpolated for display purposes, is consistent with the resolution limit, ~ 60 nm, set by the angular extent of the CCD detector. We also performed a few more reconstructions from the diffraction pattern with different initial phases, and found that the convergence speed is somewhat different in each case.

FIGURE 4. A high quality reconstruction from the diffraction pattern (after 400 iterations).

4. CONCLUSION

We believe that the successful recording and reconstruction of the test object opens a door for high-resolution three dimensional imaging of biological cells and complex sub-cellular biological structure without high resolution X-ray optics. To get 3D images, we have to record a series of diffraction patterns by rotating the specimen perpendicular to the beam, which will increase radiation damage to the specimen. We hope to circumvent this problem by using cryogenic technique of cooling the specimen down to liquid nitrogen temperature. Previous experiments have shown that biological specimens at this temperature can stand up to 10^{10} Gy dosage without observable morphological damage^{14,15}.

ACKNOWLEDGEMENTS

The decision to try oversampling as a phasing technique was arrived at in a conversation in the late 1980s with G. Bricogne. W. Yun and H. N. Chapman also participated in early parts of this experiment. These contributions are gratefully acknowledged. We are grateful to C. Jacobsen for his help and advice especially with the numerical reconstruction. We thank him and M. Howells for use of the apparatus in which the exposures were made, and S. Wirick for her assistance in the data acquisition. P. Charalambous thanks the Leverhulme Trust Great Britain for supporting the nanofabrication program at King's College, London. This work was carried out at the National Synchrotron Light Source, which is supported by the Department of Energy. Our work is supported in part by grant # DE-FG02-89ER60858 from the Department of Energy.

REFERENCES

1. Kirz, J., Jacobsen, C., and Howells, M., *Q. Rev. Biophys.* **28**, 33-130 (1995).
2. Sayre, D., and Chapman, H. N., *Acta Cryst. A* **51**, 237-252 (1995).
3. Jacobsen, C., Kirz, J., and Williams, S., *Ultramicroscopy* **47**, 55-79 (1992).
4. Thieme, J., Schmahl, G., Umbach, E., and Rudolph, D. (eds), *X-ray Microscopy and Spectromicroscopy*, Berlin: Springer-Verlag, 1998.
5. Sayre, D., "Prospects for long-wavelength x-ray microscopy and diffraction" in *Imaging Processes and Coherence in Physics*, edited by Schlenker, M. et al, Springer, Berlin, 1980, pp. 229-235.
6. Sayre, D., Chapman, H. N., and Miao, J., *Acta Cryst. A* **54**, 233-239 (1998).
7. Yun, W. B., Kirz, J., and Sayre, D., *Acta Cryst. A* **43**, 131-133 (1987).
8. Miao, J., Charalambous, C., Kirz, J., and Sayre, D., *Nature* **400**, 342-344 (1999).
9. Bates, R. H. T., *Optik* **61**, 247-262 (1982).
10. Miao, J., Sayre, D., and Chapman, H. N., *J. Opt. Soc. Am. A* **15**, 1662-1669 (1998).
11. Miao, J., Chapman, H.N., and Sayre, D., *Microscopy and Microanalysis* **3** (supplement 2), 1155-1156 (1997).
12. Miao, J., and Sayre, D., "Solving the Phase Problem by Using the Oversampling Technique," in preparation.
13. Fienup, J. R., *Appl. Opt.* **21**, 2758-2769 (1982).
14. Schneider, G., and Niemann, B., "Cryo X-ray microscopy experiment with the X-ray microscope at BESSY." in *X-ray Microscopy and Spectromicroscopy*, edited by Thieme, J., Schmahl, G., Umbach, E., and Rudolph, D., Berlin: Springer-Verlag, 1998, pp. 25-34.
15. Maser, J. et al., "Development of a cryo scanning x-ray microscope at the NSLS." in *X-ray Microscopy and Spectromicroscopy*, edited by Thieme, J. et al., Berlin: Springer, 1998, pp. 35-44.